

1 ***Electronic supporting information***
2

3 **Tailorable cellulose II nanocrystals (CNC II) prepared in**
4 **mildly acidic lithium bromide trihydrate (MALBTH)**
5
6

7 Ning Li^{1†}, Huiyang Bian^{2,3}, J.Y. Zhu³, Peter N. Ciesielski⁴, Xuejun Pan^{*,1}
8

9 1. Department of Biological Systems Engineering, University of Wisconsin-Madison, Madison,
10 WI 53706, USA

11 2. Jiangsu Co-Innovation Center of Efficient Processing and Utilization of Forest Resources,
12 Nanjing Forestry University, Nanjing, JS 210037, China

13 3. Forest Products Laboratory, U.S. Forest Service, U.S. Department of Agriculture, Madison, WI
14 53726, USA

15 4. Bioscience Center, National Renewable Energy Laboratory, Golden, CO 80401, USA

16 †. Present address: State Key Laboratory of Catalysis (SKLC), Dalian National Laboratory for
17 Clean Energy (DNL), Dalian Institute of Chemical Physics (DICP), Chinese Academy of
18 Sciences, Dalian 116023, China

19

20 Corresponding Author

21 *Tel.: +1-608-2624951; Fax: +1-608-2621228; E-mail: xpan@wisc.edu
22

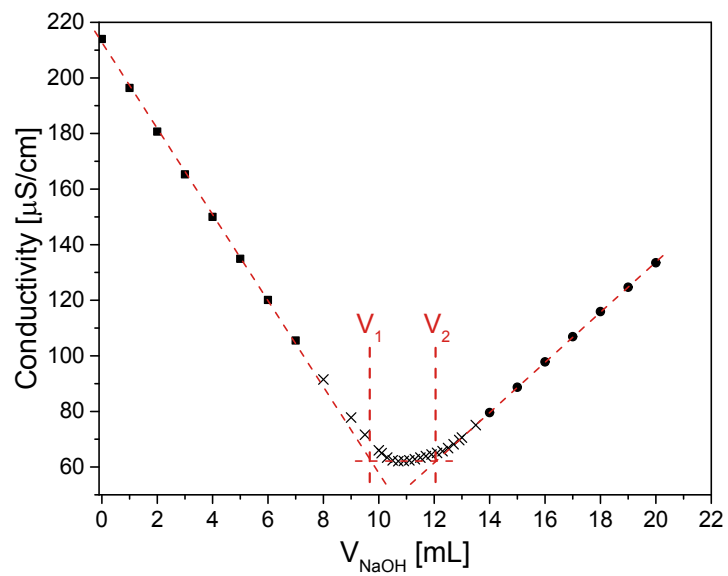
23 **List of Figures**

24

25 **Figure S1.** An electric conductivity titration curve for determining the carboxyl content in ox-
26 CNC II.3
27 **Figure S2.** POM images of the original BKP (A), swollen BKP in LBTH (B), CHR from the
28 MALBTH treatment of BKP (C, 10 min and D, 20 min).4
29 **Figure S3.** FTIR spectra of the CHR prepared in mildly acidic lithium bromide trideuterate (A)
30 and mildly acidic lithium bromide trihydrate (B).5
31 **Figure S4.** The FTIR spectra of BKP, BKP swelled in LBTH, and CHR prepared from BKP in the
32 MALBTH.6
33 **Figure S5.** The SEM image of precipitated residues collected from the ox-CNC II suspension by
34 centrifugation at 4000 rpm for 20 min.7
35 **Figure S6.** No polymorph transformation was detected during the APS oxidation verified by XRD
36 analysis.8
37 **Figure S7.** AFM height images of ox-CNC II from CHR (15 min MALBTH treatment) and
38 thickness distribution at 0.1 M APS (a and b) and 0.6 M APS (c and d).9
39 **Figure S8.** Pictures of ox-CNC II suspensions showing the Tyndall effect with laser light passing
40 through (A) and the colloidal stability after 6 months (B).10

41

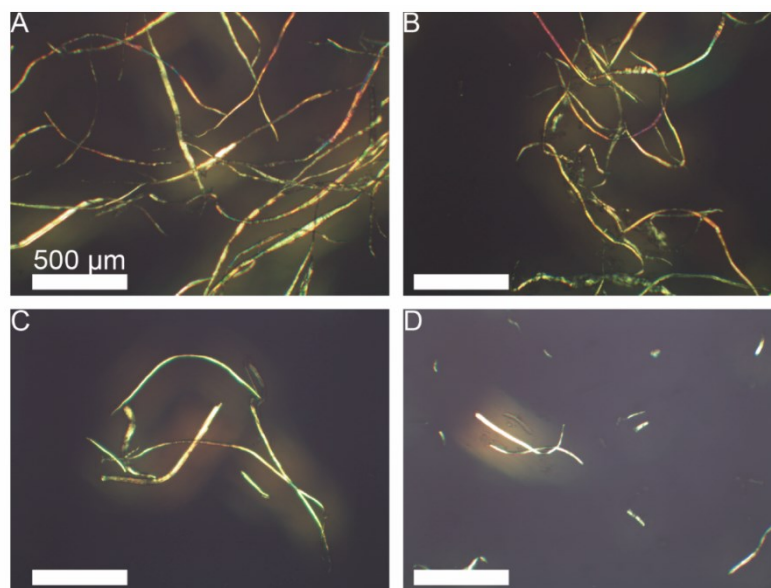
42



43

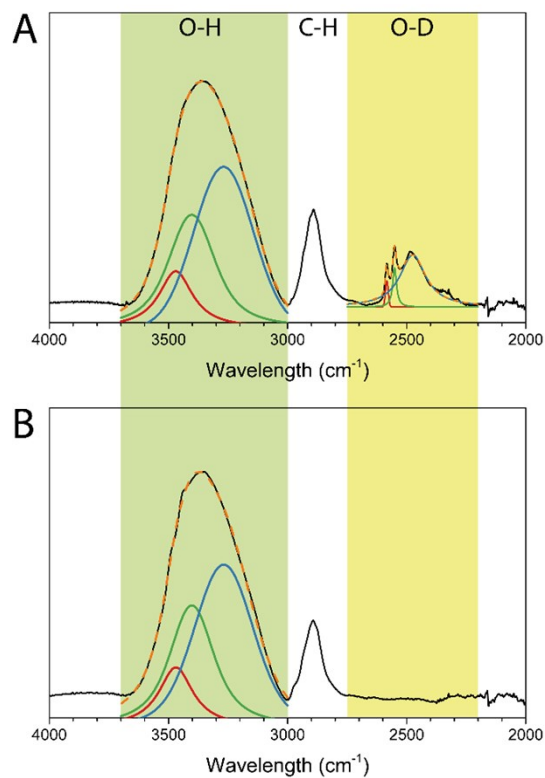
44 **Figure S1.** An electric conductivity titration curve for determining the carboxyl content in ox-
45 CNC II.

46

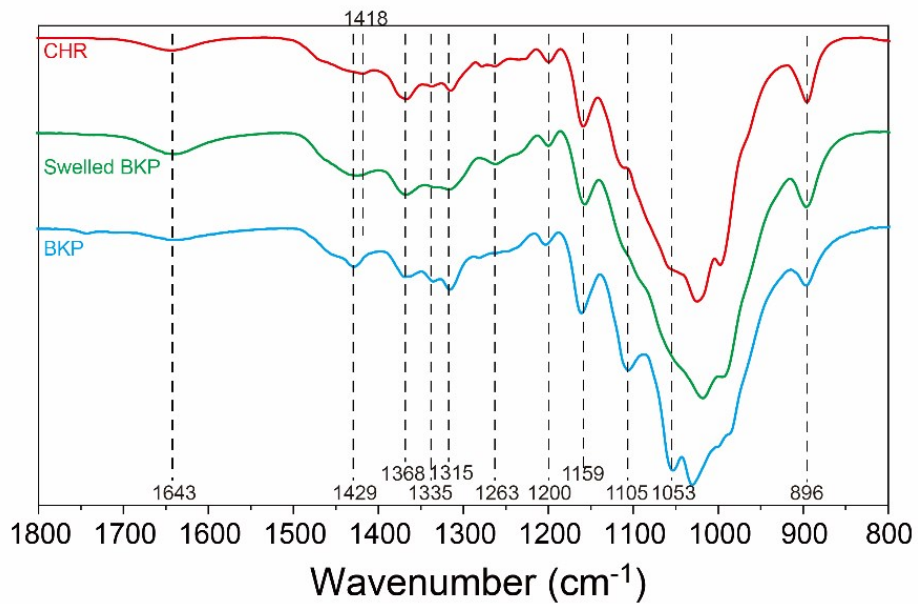


47
48
49
50
51
52

Figure S2. POM images of the original BKP (A), swollen BKP in LBTH (B), CHR from the MALBTH treatment of BKP (C, 10 min and D, 20 min). Scale bar: 500 μm

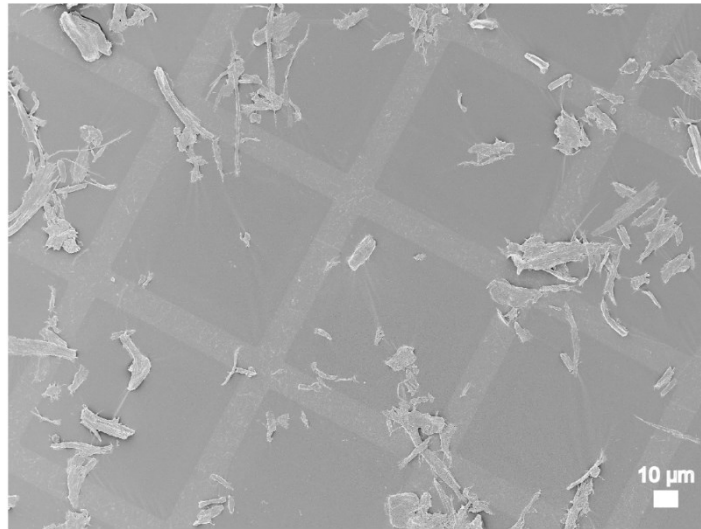


53
 54 **Figure S3.** FTIR spectra of the CHR prepared in mildly acidic lithium bromide trideuterate (A)
 55 and mildly acidic lithium bromide trihydrate (B). Note: The FTIR spectra were baseline-corrected
 56 and deconvoluted based on the Voigt peak function using Origin 2016 software.
 57
 58



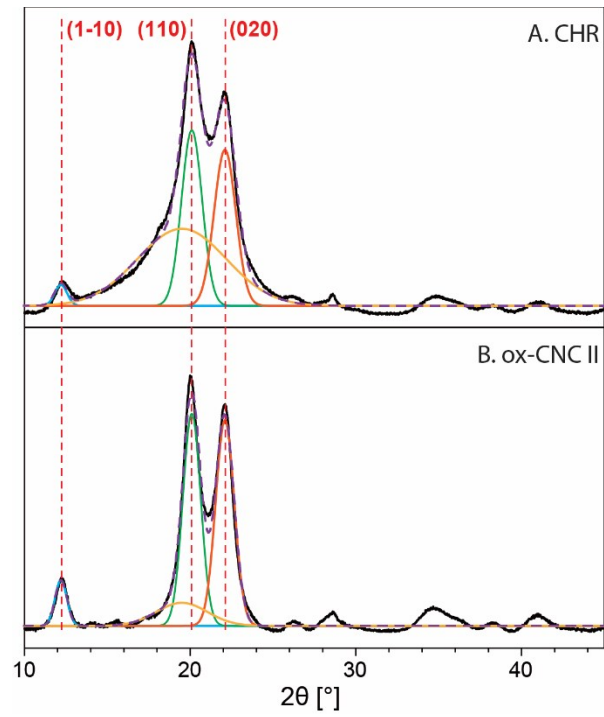
59
 60 **Figure S4.** The FTIR spectra of BKP, BKP swelled in LBTH, and CHR prepared from BKP in the
 61 MALBTH.
 62
 63

64

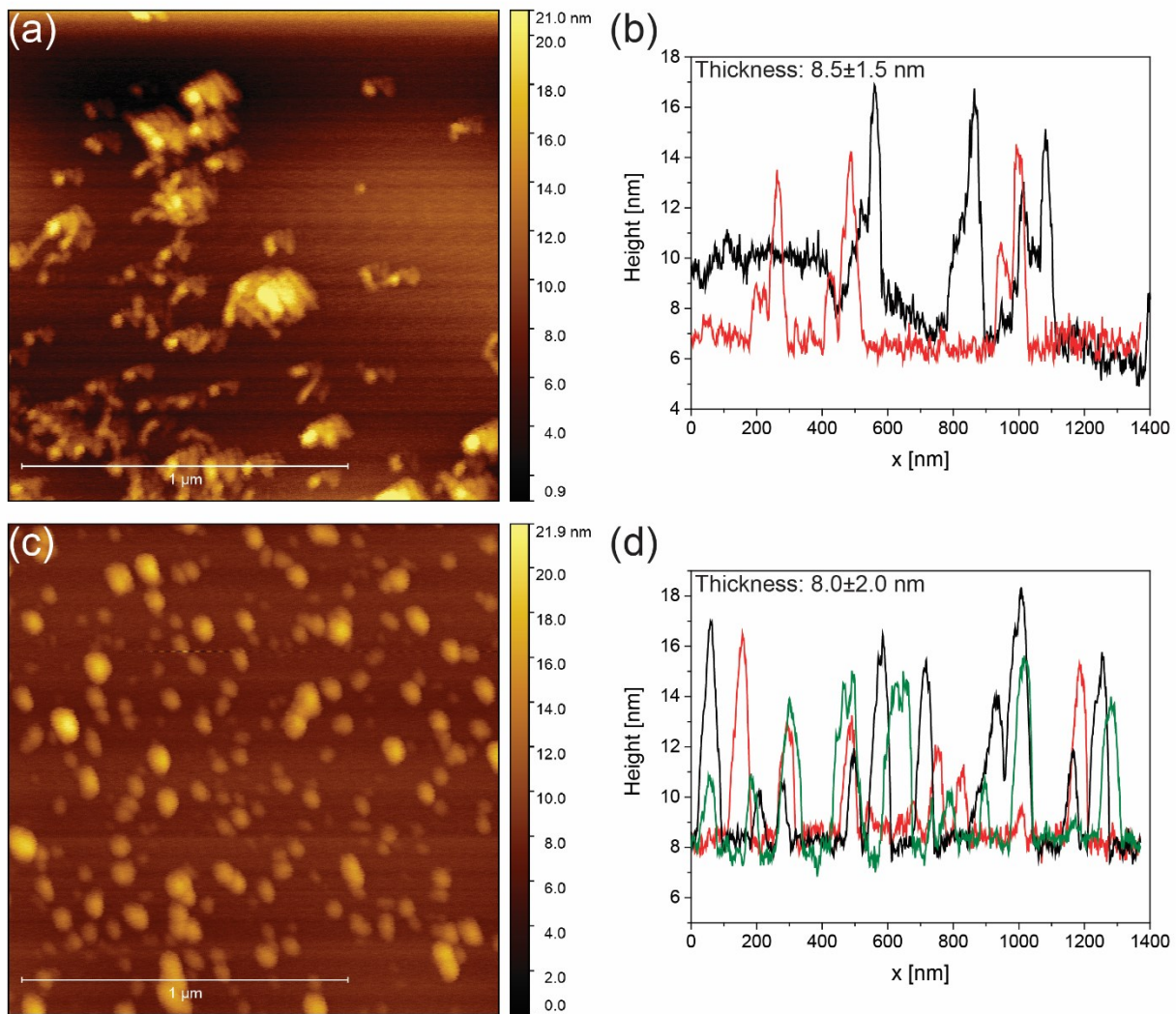


65

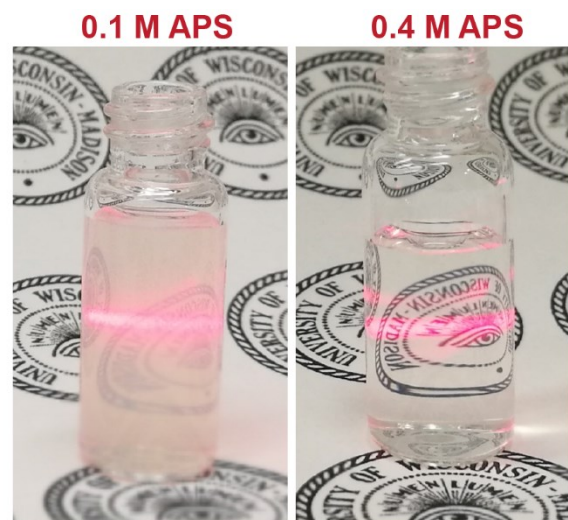
66 **Figure S5.** The SEM image of precipitated residues collected from the ox-CNC II suspension by
67 centrifugation at 4000 rpm for 20 min.



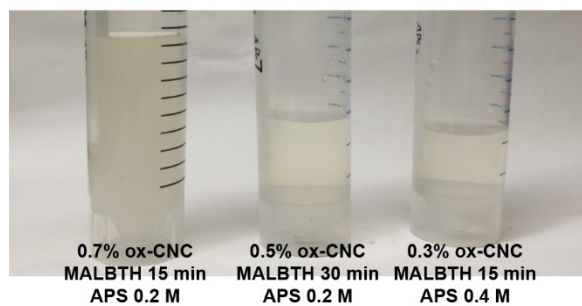
68
69 **Figure S6.** No polymorph transformation was detected during the APS oxidation verified by
70 XRD analysis.
71



72
 73 **Figure S7.** AFM height images of ox-CNC II from CHR (15 min MALBTH treatment) and
 74 thickness distribution at 0.1 M APS (a and b) and 0.6 M APS (c and d).
 75



Dispersibility after 6 months



76
77
78
79

Figure S8. Pictures of ox-CNC II suspensions showing the Tyndall effect with laser light passing through (A) and the colloidal stability after 6 months (B).